Supporting Information for

Material genome explorations and new phases of two-dimensional MoS_2, WS_2 and ReS_2 monolayers

Zhanghui Chen and Lin-Wang Wang*

Materials Sciences Division, Lawrence Berkeley National Laboratory, One Cyclotron Road, Mail Stop 50F, Berkeley, California 94720, United States

E-mail: lwwang@lbl.gov

Atomic structures of selected phases

Besides the structures in Figure 1, we have provided the atomic structures of several other selected phases in Figure S1, S2 and S3. Note that all the eighteen structures in Figure 1 are stable while some structures in Figure S1, S2 and S3 could have imaginary frequencies.

Phonon spectrum

Phonon spectrum calculations have been performed for a few selected phases of MoS_2, WS_2 and ReS_2, using the small displacement method by the PHON program.[1] A unit cell with 108 atoms is adopted in each calculation. The results for twelve phases (thirty four structures in total) are plotted in Figure S4 and S5. It should be noted that there could be

some numerical errors due to the calculation accuracy (most from the insufficient number of grid points in the FFT-mesh). We fixed these errors around zero frequency region in lower-most acoustic modes by quadratic fitting.

Molecular dynamic simulations

We have performed molecular dynamics (MD) simulations for several selected phases at different temperatures. To illustrate the structure dynamics, we have plotted the evolution of the total energy, pair distribution function and atomic moving function.

The pair distribution function is defined as:

$$\rho'(r,t) = \sum_{i=1}^{N} \sum_{j=1, j\neq i}^{N} \delta\left(r - R_{ij}(t)\right) \tag{1}$$

where N is the number of atoms; $R_{ij}(t)$ is the distance between the atom i and atom j at the periodic image at the time t. In order to have a smooth function, the sigma function here is broadened by a Gaussian smearing and has the following form:

$$\delta\left(r - R_{ij}\right) = \frac{1}{\sigma\sqrt{2\pi}} \exp\left[-\frac{\left(r - R_{ij}\right)^2}{2\sigma^2}\right] \tag{2}$$

The broadening parameter σ is set to 0.1 Å.

The atomic moving function is used to show the atomic movement during the MD process. It is defined as:

$$s'(r,t) = \sum_{i=1}^{N} \delta\left(\left|R_i(t) - R_i(0)\right|\right) \tag{3}$$

where $R_i(t)$ is the position of the atom i at the time t. The movement $|R_i(t) - R_i(0)|$ is calculated at the periodic image. The sigma function is also broadened by the Gaussian smearing of Formula (2).

The above functions might not be smooth enough when N is small. To further smooth them and show the mean values around the time region Δt, we define the mean pari distri-

bution function and the mean atomic correlation function as:

$$\rho(r,t) = \int_{t-\Delta t/2}^{t+\Delta t/2} \rho'(r,t')dt' \tag{4}$$

$$s(r,t) = \int_{t-\Delta t/2}^{t+\Delta t/2} s'(r,t')dt' \tag{5}$$

Δt here is set to 200 fs.

The results for H-MoS_2, T_1'-MoS_2 and T_2'-MoS_2 are plotted in Figure S6, S7 and S8, respectively. Note the simulations at 2000K are used to study the funnel feature at a short time. In reality, this temperature is higher than the melting point. We can see that the $\rho(r,t)$ and $s(r,t)$ curves at 0 ps are different from other curves after a certain-time simulation. This is because the structure at 0 ps is the local minimum at zero temperature and the dynamics have not reached equilibrium at the simulated temperature.

Properties of selected phases

We have studied the electronic properties of several selected phases when they are doped or packed into bulk, using HSE06 exchange-correlation functional.

Figure S9 shows the atomic structures and electronic band structure of the 42-WS_2 bulk. Its band structure is similar to the corresponding monolayer with slightly shifted and distorted bands. The direct band gap in the Γ point still exists but decreases to a much smaller value (0.005 eV).

Figure S10 shows the packing of the $Pmm2$-WS_2 monolayer. Since its lower side (noted as "A" side) and upper side (noted as "B" side) are different, it can have two types of packing, i.e., ABAB and ABBA. The band structure of the ABAB bulk is similar to the monolayer. The ABBA bulk is more different, where each band splits into two bands due to symmetry breaking. The crossing bands (Dirac cone) exist in both types of bulk.

Figure S11 compares the band structures of T_1'-phase and T_2'-phase of MoS_2 and WS_2

at -1.0 electron doping and 0.5 hole doping. Their differences between MoS_2 and WS_2 are clearer than the situation without doping.

Charge doping with different vacuum thicknesses

In our DFT calculations, the charge doping is applied by a homogeneous background charge. We thus concern the effect of the vacuum thickness. We have calculated the energy difference (ΔE) between T_1'-MoS_2 and H-MoS_2 at different lengths of the supercell out-of-plane axis, as shown in Figure S12. We find that, at a small charge doping, ΔE keeps almost the same among different vacuum thicknesses. The overall trend of the ΔE curve also keeps unchanged at a large charge doping. Thus, it is reasonable to use ΔE to indicate the possible phase transition motivated by charge doping.

References

(1) Alfè, D. PHON: A program to calculate phonons using the small displacement method. *Comput. Phys. Commun.* **2009**, *180*, 2622–2633.

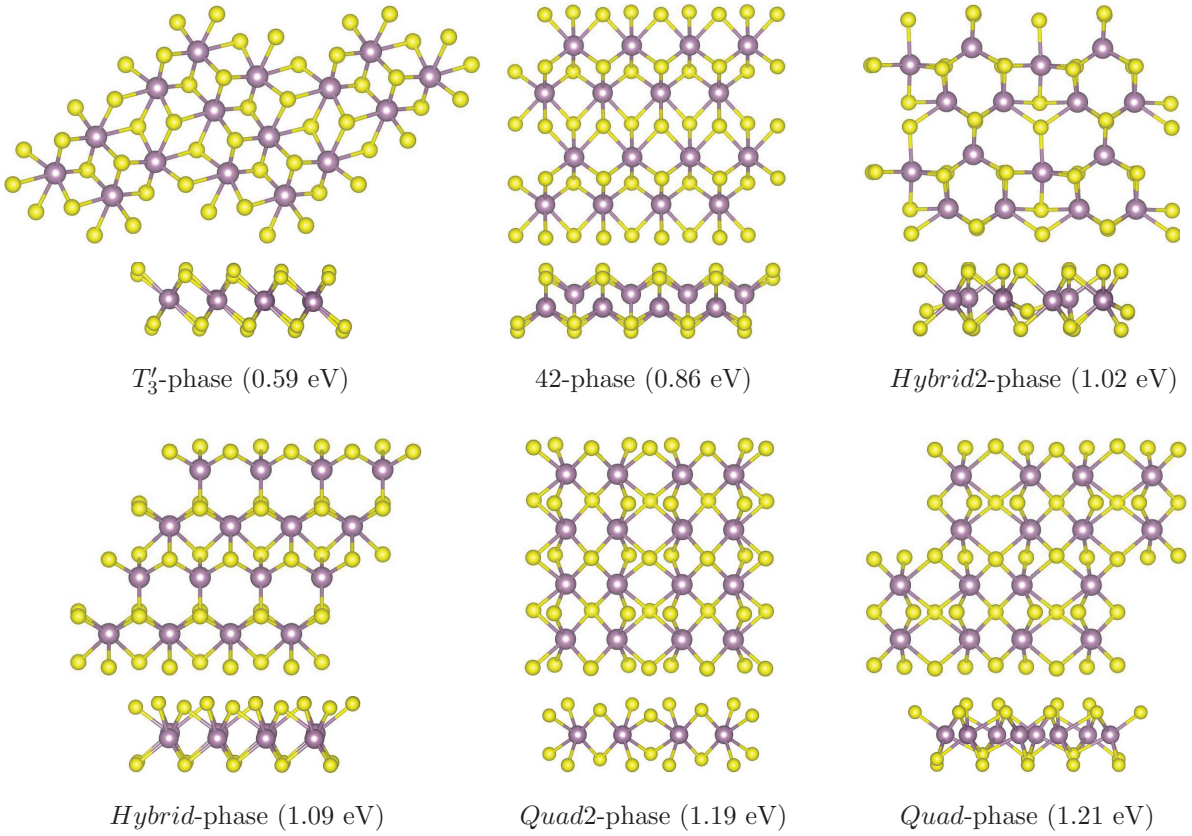

Figure S1: Atomic structures of several selected phases of 2D MoS_2 monolayers at the top view and side view. The phases are arranged with the energy from low to high. Note that T_3', 42, *Quad*2 and *Quad* phases are stable while *Hybrid*2 and *Hybrid* phases have imaginary frequency.

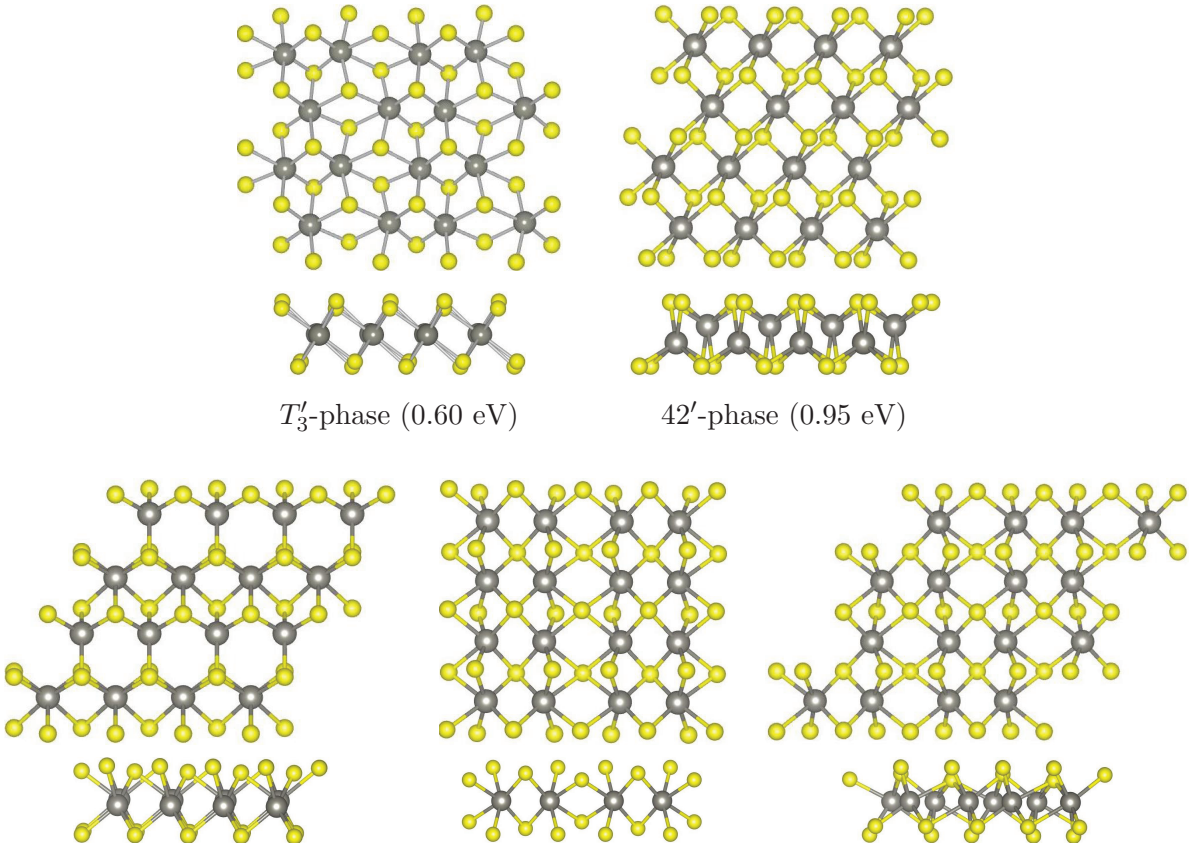

Figure S2: Atomic structures of several selected phases of 2D WS_2 monolayers at the top view and side view. The phases are arranged with the energy from low to high. Note that T_3' and *Quad* phases are stable while 42′, *Hybrid* and *Quad*2 phases have imaginary frequency. *Hybrid*2-phase does not exist in WS_2 due to non-zero forces.

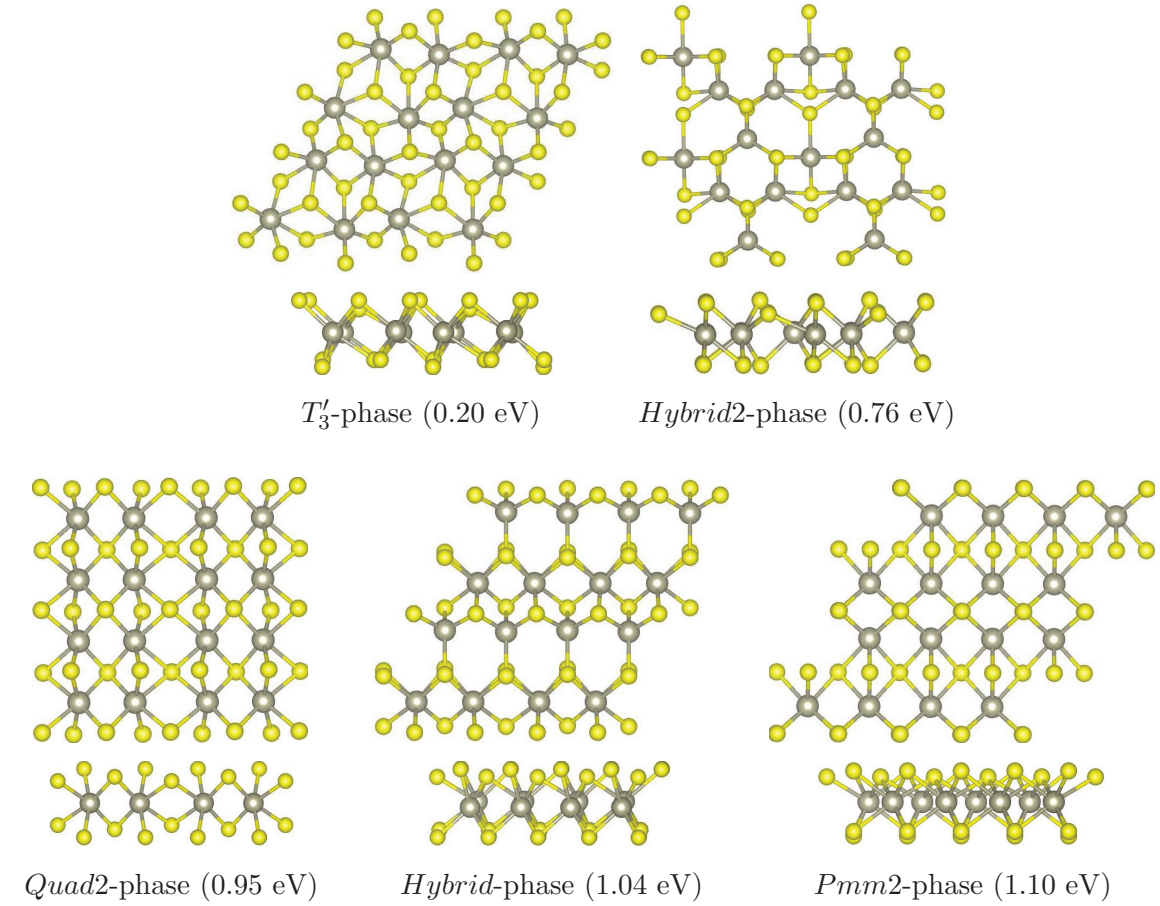

Figure S3: Atomic structures of several selected phases of 2D ReS_2 monolayers at the top view and side view. The phases are arranged with the energy from low to high. Note that T_3', $Hybrid2$ and $Hybrid$ phases are stable while $Quad2$ and $Pmm2$ phases have imaginary frequency. $42'$-phase does not exist in ReS_2 due to non-zero forces.

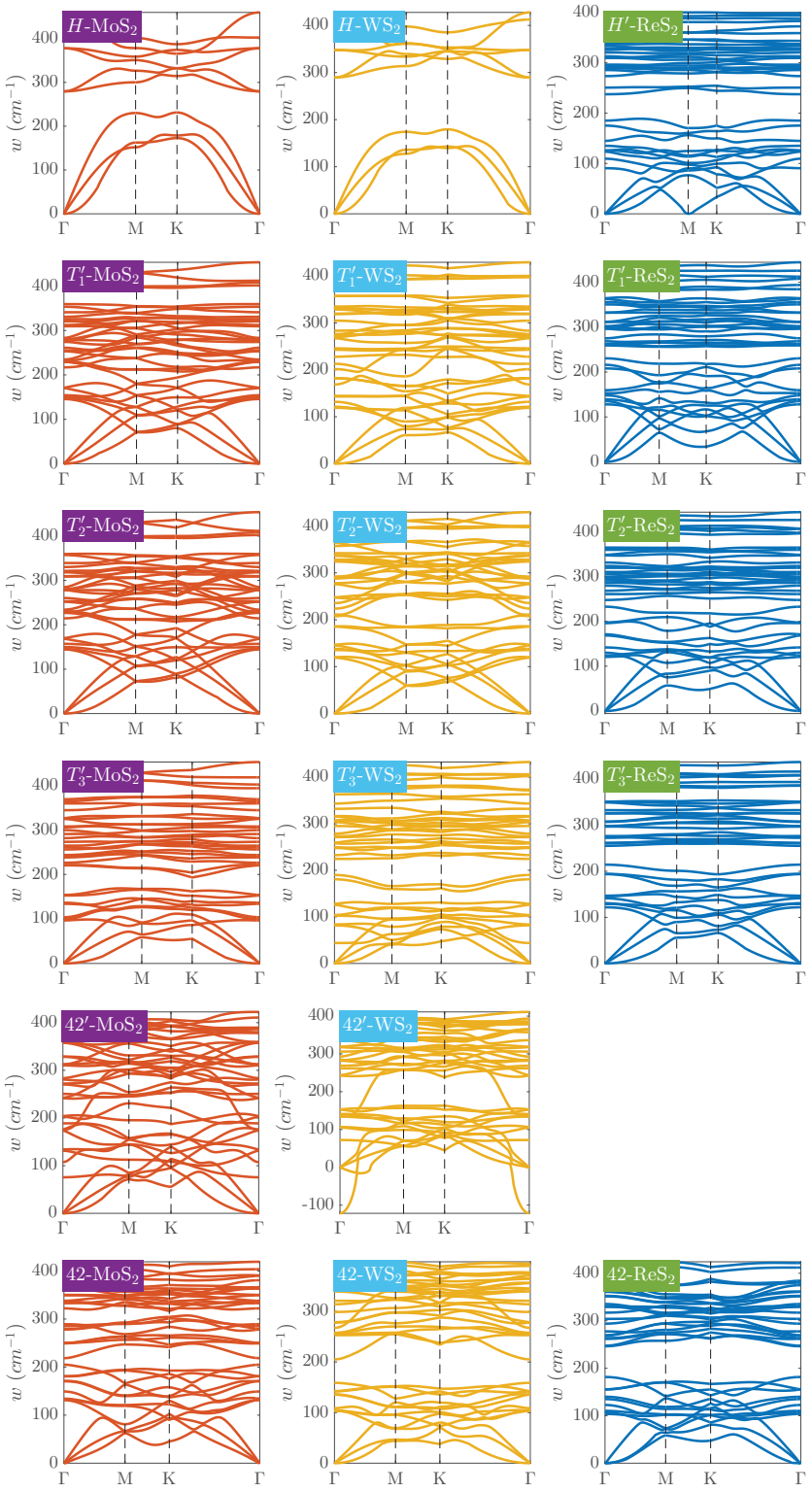

Figure S4: Phonon spectrum of several selected phases of 2D MoS_2, WS_2 and ReS_2 monolayers. The phases are arranged with their energies at the MoS_2 system from low to high. Note that H'-ReS_2 is not the global minimum but is arranged at the first row to compare with H-MoS_2 and H-WS_2. $42'$-ReS_2 does not exist due to non-zero forces.

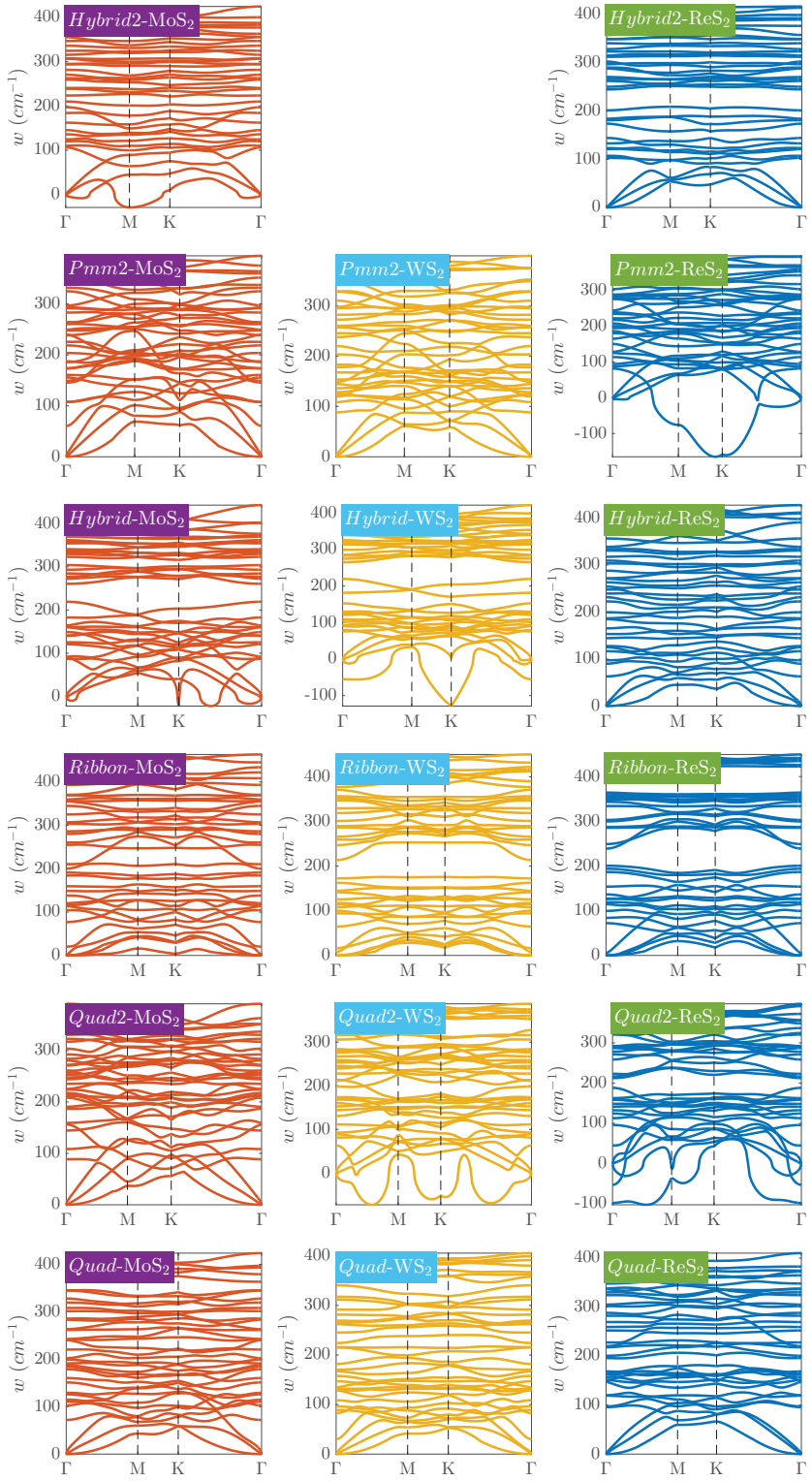

Figure S5: (Continued) Phonon spectrum of several selected phases of 2D MoS_2, WS_2 and ReS_2 monolayers. The phases are arranged with their energies at the MoS_2 system from low to high. Note that *Hybrid*2-WS_2 does not exist due to non-zero forces.

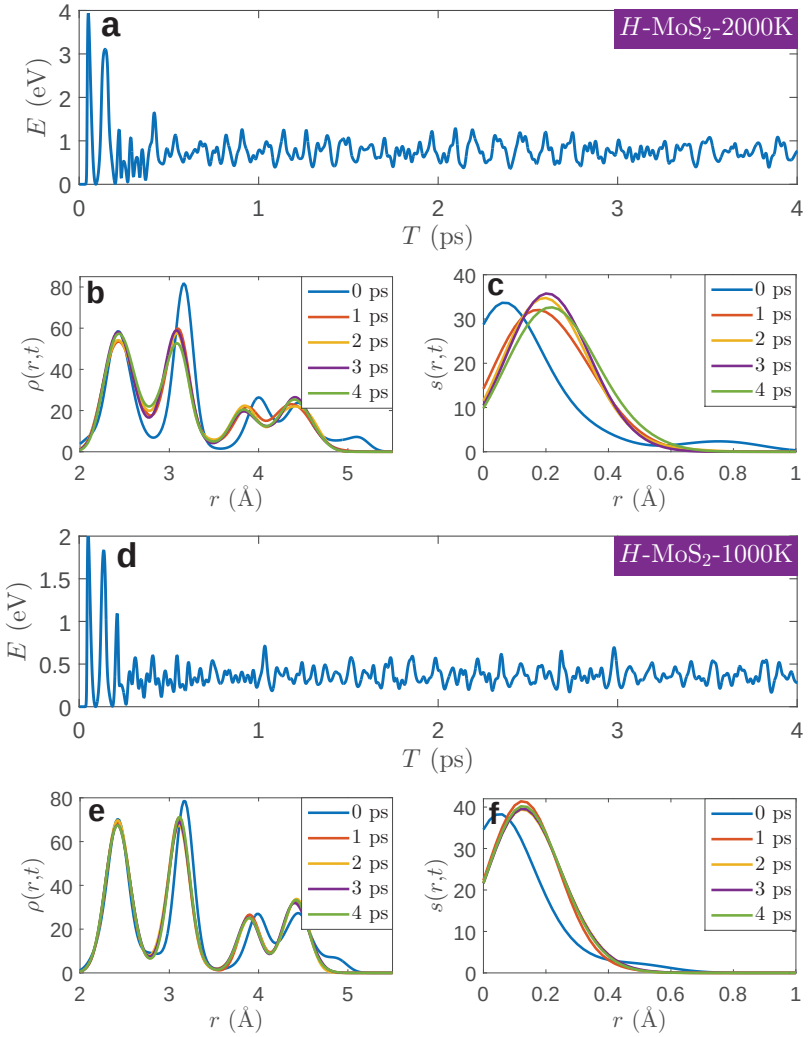

Figure S6: Molecular dynamics simulations for H-phase MoS_2 at (a-c) 2000K and (d-f) 1000K. Panel a and d are the evolution of the total energy (per formula unit) relative to the original structure; panel b and e are the evolution of pair distribution function; panel c and f are the evolution of atomic moving function.

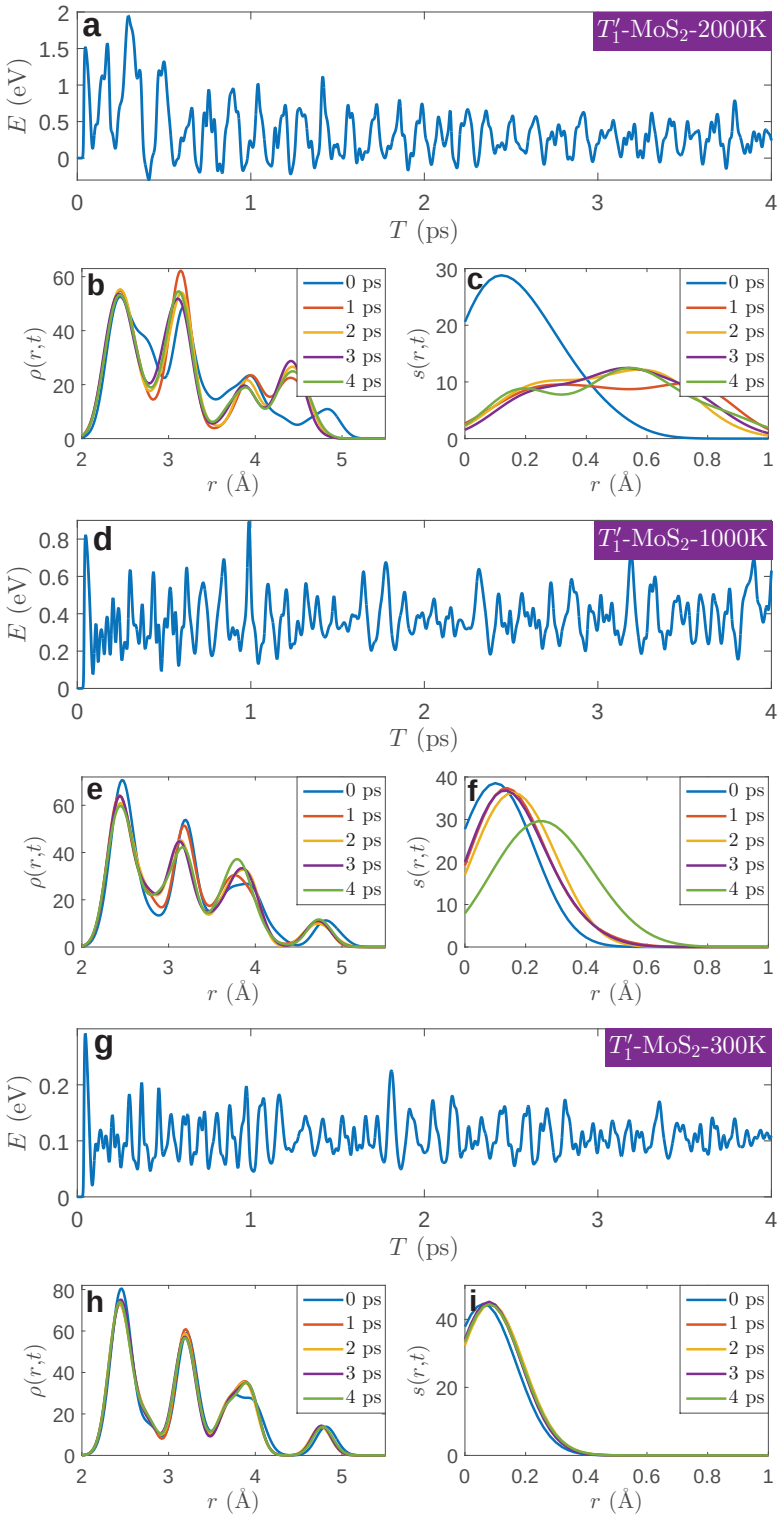

Figure S7: Molecular dynamics simulations for T_1'-phase MoS_2 at (a-c) 2000K, (d-f) 1000K and (g-i) 300K. Panel a, d and g are the evolution of the total energy (per formula unit) relative to the original structure; panel b, e and h are the evolution of pair distribution function; panel c, f and i are the evolution of atomic moving function.

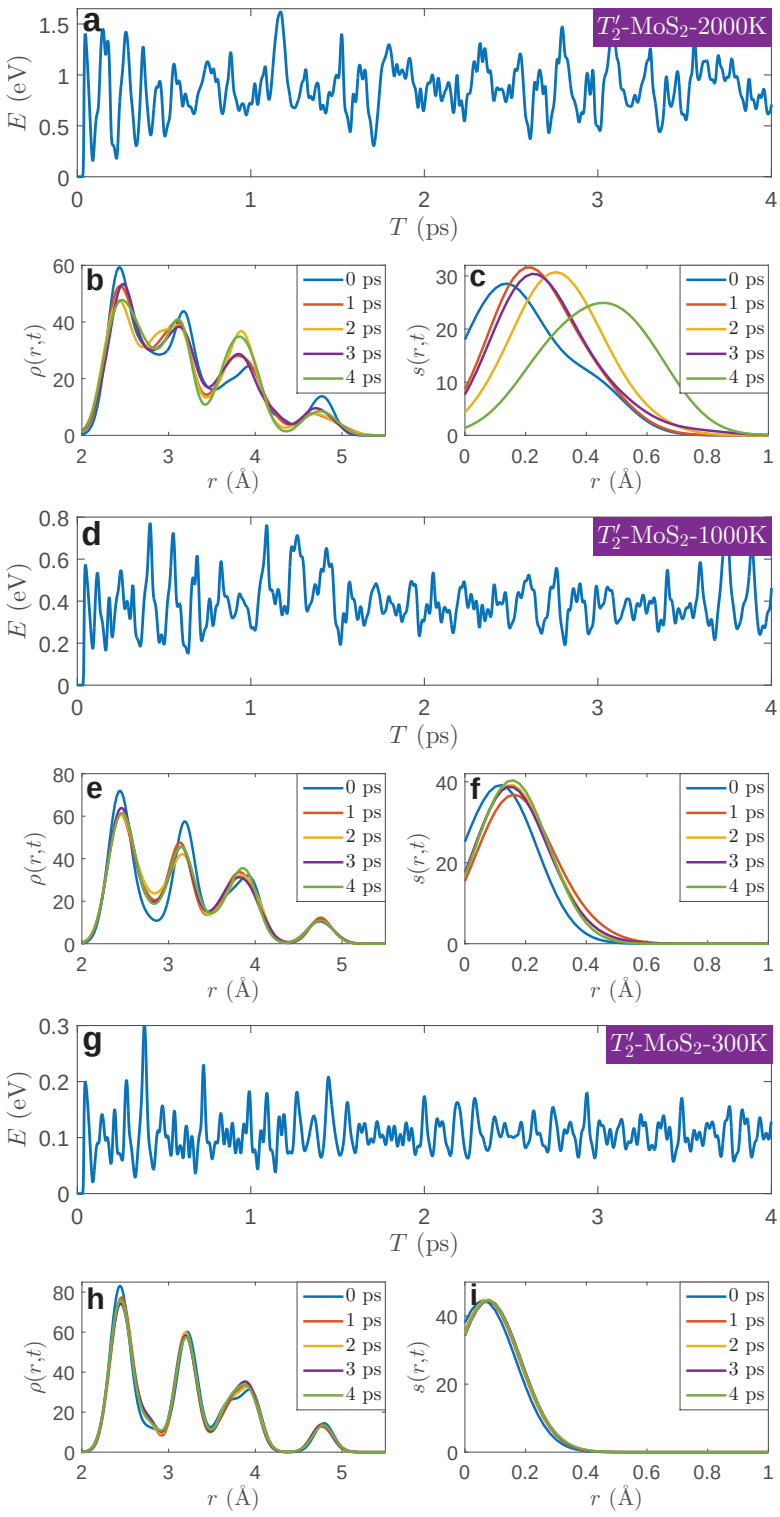

Figure S8: Molecular dynamics simulations for T_2'-phase MoS_2 at (a-c) 2000K, (d-f) 1000K and (g-i) 300K. Panel a, d and g are the evolution of the total energy (per formula unit) relative to the original structure; panel b, e and h are the evolution of pair distribution function; panel c, f and i are the evolution of atomic moving function.

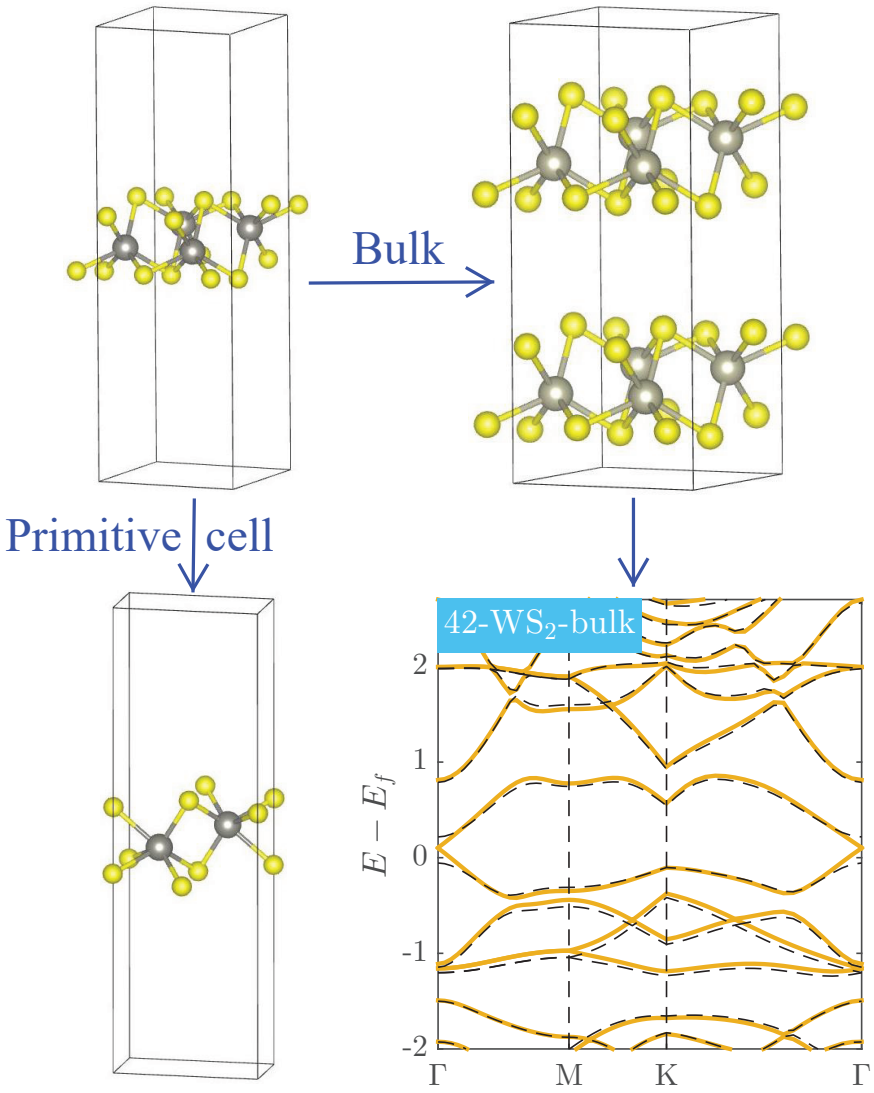

Figure S9: Atomic structures and electronic band structures of 42-WS_2 packed into the bulk. The gray atoms are W and the yellow atoms are S. The black dashed line in the band structures is for the 42-WS_2 monolayer as the reference. The yellow line is for the bulk. The Fermi level (E_f) is set to the zero energy of the y axis.

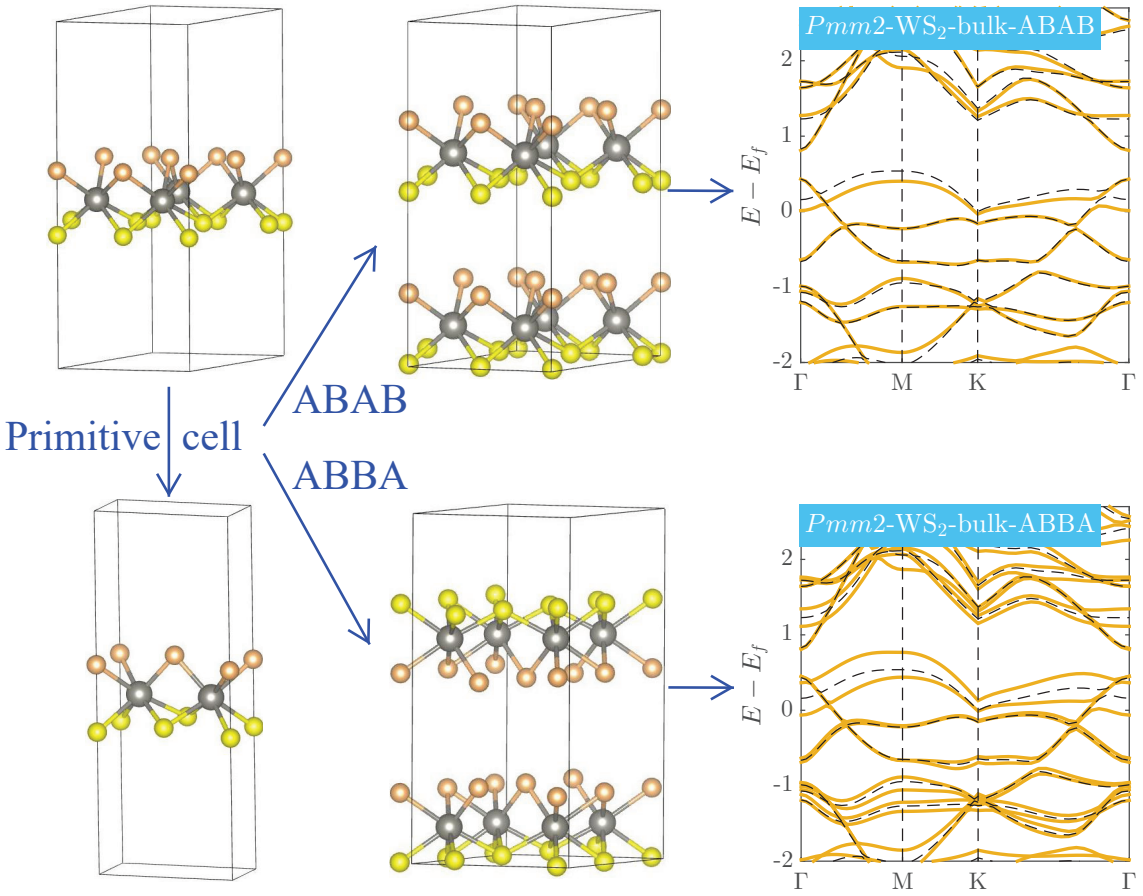

Figure S10: Atomic structures and electronic band structures of $Pmm2$-WS_2 packed into the bulk with two different ways (i.e., ABAB and ABBA). The gray atoms are W; both the yellow ("A" side) and gold atoms ("B" side) are S. The black dashed line in the band structures is for the $Pmm2$-WS_2 monolayer as the reference. The yellow line is for the bulk. The Fermi level (E_f) is set to the zero energy of the y axis.

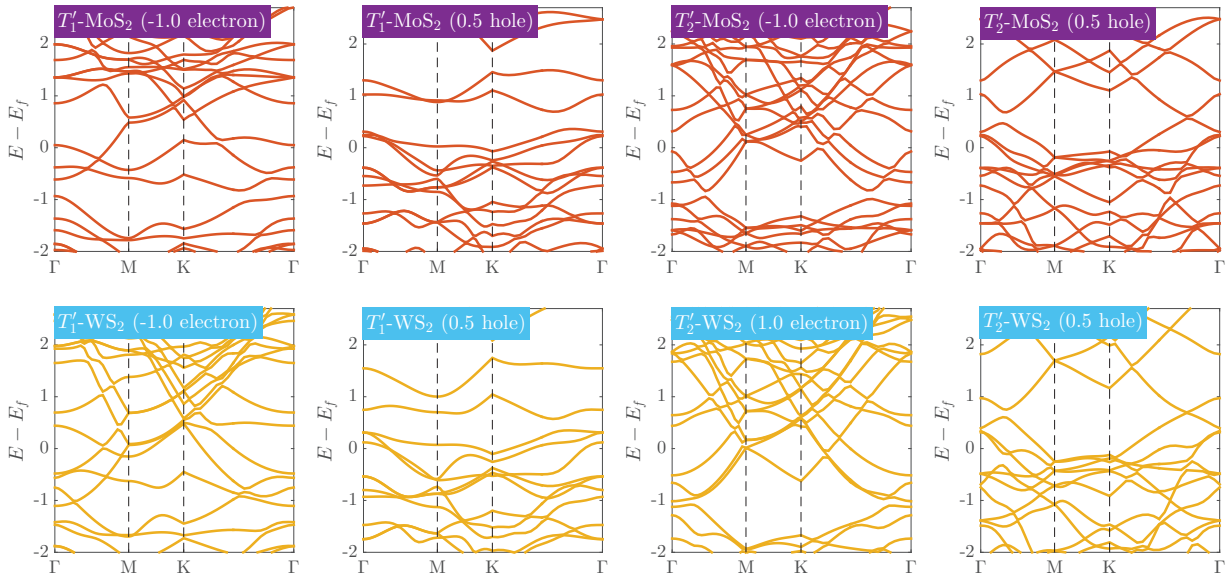

Figure S11: Band structures of T_1'-phase and T_2'-phase of MoS_2 and WS_2 at electron and hole doping (in the unit of e/MoS_2 and e/WS_2). The Fermi level (E_f) is set to the zero energy of the y axis.

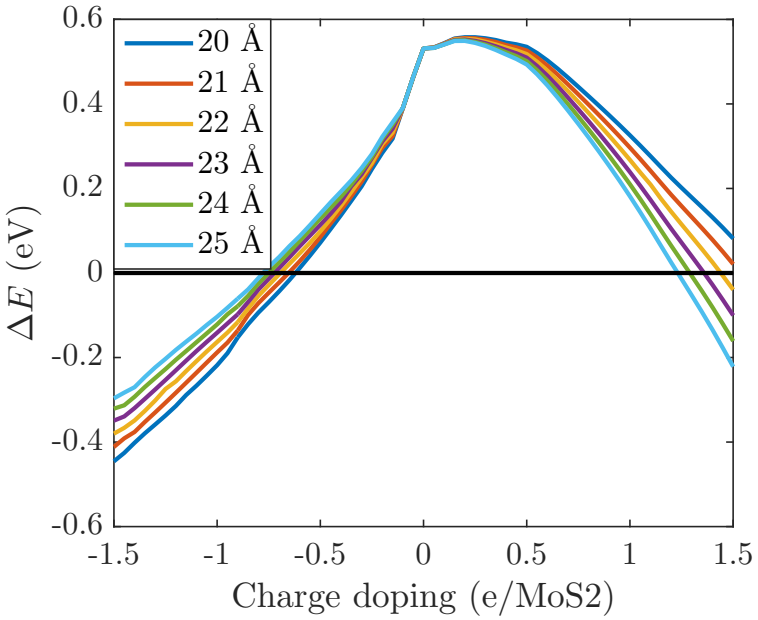

Figure S12: Energy difference (ΔE) between T_1'-MoS_2 and H-MoS_2 as a function of charge doping. Negative charge in the x axis means electron doping and positive charge means hole doping. Different curves represent different lengths of the supercell out-of-plane axis. The black referenced line illustrates the zero energy.